

## Epidemic dynamics on information-driven adaptive networks

Zhan, Xiuxiu; Liu , Chuang ; Sun, Gui-Quan; Zhang , Zi-Ke

**DOI**

[10.1016/j.chaos.2018.02.010](https://doi.org/10.1016/j.chaos.2018.02.010)

**Publication date**

2018

**Document Version**

Accepted author manuscript

**Published in**

Chaos, Solitons and Fractals

**Citation (APA)**

Zhan, X., Liu , C., Sun, G.-Q., & Zhang , Z.-K. (2018). Epidemic dynamics on information-driven adaptive networks. *Chaos, Solitons and Fractals*, 108, 196-204. <https://doi.org/10.1016/j.chaos.2018.02.010>

**Important note**

To cite this publication, please use the final published version (if applicable). Please check the document version above.

**Copyright**

Other than for strictly personal use, it is not permitted to download, forward or distribute the text or part of it, without the consent of the author(s) and/or copyright holder(s), unless the work is under an open content license such as Creative Commons.

**Takedown policy**

Please contact us and provide details if you believe this document breaches copyrights. We will remove access to the work immediately and investigate your claim.

# Epidemic Dynamics On Information-Driven Adaptive Networks

Xiu-Xiu Zhan<sup>a,b</sup>, Chuang Liu<sup>a,\*</sup>, Gui-Quan Sun<sup>c</sup>, Zi-Ke Zhang<sup>a,d,e,\*</sup>

<sup>a</sup>*Alibaba Research Center for Complexity Sciences, Hangzhou Normal University, Hangzhou 311121, P. R. China*

<sup>b</sup>*Faculty of Electrical Engineering, Mathematics and Computer Science, Delft University of Technology, 2628 CD Delft, The Netherlands*

<sup>c</sup>*Complex Sciences Center, Shanxi University, Taiyuan 030006, P. R. China*

<sup>d</sup>*Department of Automation, Shanghai Jiao Tong University, Shanghai 200240, P. R. China*

<sup>e</sup>*Alibaba Research Institute, Hangzhou, 311121, P. R. China*

---

## Abstract

Research on the interplay between *the dynamics on the network* and *the dynamics of the network* has attracted much attention in recent years. In this work, we propose an information-driven adaptive model, where disease and disease information can evolve simultaneously. For the information-driven adaptive process, susceptible (infected) individuals who have abilities to recognize the disease would break the links of their infected (susceptible) neighbors to prevent the epidemic from further spreading. Simulation results and numerical analyses based on the pairwise approach indicate that the information-driven adaptive process can not only slow down the speed of epidemic spreading, but can also diminish the epidemic prevalence at the final state significantly. In addition, the disease spreading and information diffusion pattern on the lattice give a visual representation about how the disease is trapped into an isolated field with the information-driven adaptive process. Furthermore, we perform the local bifurcation analysis on four types of dynamical regions, including healthy, a continuous dynamic behavior, bistable and endemic, to understand the evolution of the observed dynamical behaviors. This work may shed some

---

\*Corresponding author

*Email addresses:* liuchuang@hznu.edu.cn (Chuang Liu), zhangzike@gmail.com (Zi-Ke Zhang)

lights on understanding how information affects human activities on responding to epidemic spreading.

*Keywords:* Epidemic spreading, Information diffusion, Adaptive model, Bifurcation analysis

---

## 1. Introduction

The spreading dynamic is one of the core issues in network science [1, 2], where most of the related researches focus on epidemic spreading and information diffusion in recent years. Much of the work to date focuses on the analysis of these two processes independently, such as the spread of single contagion [3] or concurrent diseases [4, 5], and the diffusion of various kinds of information (e.g., news [6], rumor [7], innovation [8].). However, the epidemic spreading process is closely coupled with the corresponding disease information diffusion (or saying awareness) in the real world. For instance, during the severe acute respiratory syndrome (SARS) outbreak in China in 2003, overwhelming number of disease reports have been posted. These kind of information about SARS may affect the individuals' behavior in keeping away from SARS and thus help to make the disease under control [9, 10]. Therefore, disease information diffusion may play an important role in the control of the epidemic outbreak, but it is not easy to quantitatively measure the strength of its impact [11].

Nowadays, some models have been proposed to model the interaction between epidemic spreading and information diffusion on complex networks [11, 12, 13, 14]. The fundamental assumption is that, when a disease starts to spread in the population, people may get the disease information from their friends or media before the advent of the epidemic and take some preventive measures to keep away from being infected [12, 15, 16]. By depicting preventive measures as the reduction of transmitting probability [17, 18] or particular states of individuals (immune or vaccination) [19], previous models showed that the disease information diffusion indeed inhibits the epidemic spreading significantly (reduce the epidemic prevalence as well as enhance the epidemic threshold) [12, 20].

Therefore, the emergence of mutual feedback between information diffusion and epidemic spreading [11] exhibits the intricate interplay between these two types of spreading dynamics. The interplay between these two types of spreading dynamics is similar to the competing epidemics [21, 22] to some extent, that is to say, there is a competitive mechanism between epidemic spreading and the information diffusion. Most of aforementioned studies of such complex interacted spreading dynamics are based on static network, i.e., the network structure stays fixed when the two processes are spreading on the network. However, individuals would sometimes cut off the connections with the infected ones when they are aware of the disease, leading to the change of network structure. Consequently, how to characterize the mutual spreading process on the adaptive networks is a crucial issue we want to address in this work.

Generally, the network dynamic researches could be classified into two lines: (i) one is the *dynamics of the network*, which focuses on the time evolution of network structure [23, 24, 25]; (ii) the other is considered as the *dynamics on the network*, which concerns the state change of the nodes (or interactions) on networks, such as the epidemic spreading and information diffusion process [26, 27], the evolutionary game [28] and so forth. Currently, researchers became to study how the epidemic would spread on adaptive networks, i.e., considering one epidemic spreading process on dynamical changing networks [29]. In [29], the author proposed a model by considering that the susceptible individuals are allowed to protect themselves by rewiring their links from the infected neighbors to some other susceptible ones [30, 31, 32]. Many researches indicate that segregating infected (or susceptible) individuals with the adaptive behavior is an efficient strategy to reduce the fraction of susceptible-infected ( $SI$ ) interactions, as well as hinder the outbreak of the whole epidemic spreading [33, 34, 35]. In addition, abundant temporal behaviors are presented to illustrate the spreading dynamics on the adaptive network, such as the coexistence of multiple stable equilibrium and the appearance of an oscillatory region, which are absent in the spreading dynamics on static networks [29, 36]. Besides the edge rewiring strategy, the link cutting or temporarily deactivating is also a commonly used

rule in the adaptive models[37, 38].

In this work, we consider a more complicated case that two dynamical processes (i.e., epidemic spreading and disease information diffusion) are spreading  
60 on adaptive networks. Therefore, three dynamical processes are coupled in this case, we aim to illustrate how the adaptive behavior can affect the interplay between epidemic spreading and information diffusion. The adaptive behavior is aroused by the individuals awareness of the disease. In this model, those who have been informed of the emergence of disease can break their neighbouring  
65 connections to prevent further infection. Additionally, epidemic spreading and disease information diffusion are described by the SI and SIS model, respectively. The disease information generation of the infected individuals is considered to form a mutual feedback loop between these two types of spreading dynamics [17]. Therefore, the effect of information diffusion on epidemic spreading could  
70 be interpreted by two aspects: (i) reduce the epidemic spreading probability with protective measures; and (ii) cut off *SI* links with the information-driven adaptive process. Both numerical analyses based on the pairwise approach and simulation results indicate that the information diffusion and the adaptive behavior of the nodes can inhibit the epidemic outbreak significantly. In addition,  
75 we present a full local bifurcation diagram to show the abundant dynamical behaviors in the proposed model.

The paper is organized as follows. In Section 2, we give a detailed description of the model as well as mathematical expressions based on the mean-field model and the pairwise model. In Section 3, we first analyze the case of epidemic and disease information spreading on static network, i.e., the case of no  
80 adaptive behavior is taken into account. We further give the results of how the epidemic and disease information spreading processes interact with each other on adaptive network. The sensitivity analysis of the parameters and dynamical characterization of the model is given in the end of Section 3. We conclude the  
85 paper with some future direction of the work in Section 4.

## 2. Model

### 2.1. Model description

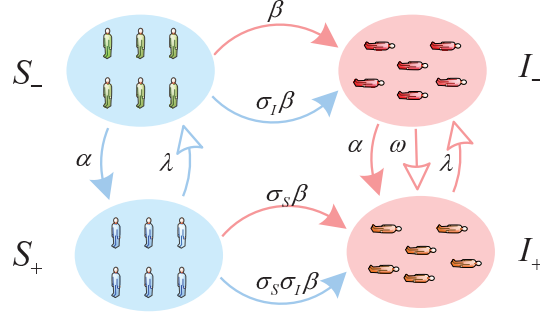


Figure 1: (Color online) Transmission diagram of epidemic spreading (*SI* model in the horizontal direction) and disease information diffusion model (*SIS* model in the vertical direction).

We give a detailed illustration of our model in Fig. 1. The vertical transformation describes the diffusion of disease information by an *SIS* model, where individuals can be at one of the two states: (i) +: indicates that the individuals have known the existence of the disease, denoted as the informed ones; (ii) -: indicates that the individuals have not known the existence of the disease. At each time step, the informed nodes will transmit the information to their unknown (-) neighbours with probability  $\alpha$ , and each informed individual may forget the information of the disease with a probability  $\lambda$ . Besides, the one who has been infected by the disease will become to know the information of the disease with a corresponding rate  $\omega$  [11, 13].

In the horizontal transformation of Fig. 1, the epidemic spreading is described by an *SI* model. Each node is at one of two states, susceptible (*S*) or infected (*I*). The disease can be transmitted through the *SI* links, where the *S*-state individuals could be infected with the probabilities  $\beta$ ,  $\sigma_I \beta$ ,  $\sigma_S \beta$  and  $\sigma_{SI} \beta$  respectively through  $S_- I_-$ ,  $S_- I_+$ ,  $S_+ I_-$  and  $S_+ I_+$  links, where  $\sigma_I, \sigma_S$  and  $\sigma_{SI}$  are the impact factors of the information on epidemic spreading. Generally, when people know the occurrence of the disease (informed individuals), they would like to take some measures to protect themselves, leading to the

reduction in infectivity ( $0 < \sigma_S, \sigma_I < 1$ ). In particular, the influence coefficient of the epidemic spreading probability through  $S_+I_+$  links could be calculated as  $\sigma_{SI} = \sigma_S\sigma_I$ , with the assumption of the independent effect of the infected probability.

110      Additionally, we consider an information-driven adaptive process which the informed individuals would reduce physical contacts to protect themselves or their friends. That is to say, the informed susceptible individuals ( $S_+$ ) will keep away from their infected neighbors to protect themselves from being infected, and informed infected individuals ( $I_+$ ) will also avoid contacting their suscep-  
 115      tible neighbors to prevent the epidemic from further spreading. Consequently, the edge-breaking rule of adaptive behavior is adopted [37]. Thus, at each time step, the  $S_+$  ( $I_+$ ) state individuals will break the links connected to their  $I$  ( $S$ )-state neighbors with rate  $r_S$  ( $r_I$ ) respectively. Specially, the breaking rate of the  $S_+I_+$  pairs could be interpreted as  $1 - (1 - r_S)(1 - r_I)$  with the inde-  
 120      pendent assumption. It is worth noting that the deactivation of  $SI$  links only represents the avoidance of physical contacts between the  $S$ - and  $I$ -state individuals. That is to say, the edge-breaking process will not affect the diffusion of disease information for it can be transmitted through other types of connections such as phone, internet and so forth. The dynamic of the epidemic spreading  
 125      degenerates to a classical SI model when we set  $r_S = r_I = 0$ , i.e., there is no edge-breaking in this case.

According to the model described above, the spreading process can be summarized as follows. At the beginning, an individual is randomly selected as the  $I_+$  node, which is considered as the *seed* of both the epidemic spreading and  
 130      information diffusion, and all other individuals are set as  $S_-$  ones. At each time step, (i) the infected individuals would transmit the disease to their susceptible neighbors with the corresponding probabilities; (ii) the informed individuals would transmit the disease information to their un-informed neighbors; (iii) the informed individuals can forget the information; (iv) the informed individual-  
 135      s would also break the links with their relevant neighbors by considering the adaptive mechanism. Finally, the spreading process would be terminated when

the size of the infected individuals becomes stable.

## 2.2. Numerical mathematical analysis

140 Firstly, we develop theoretical analyses to depict the dynamic processes of both information diffusion and epidemic spreading. In particular, mean-field analysis and the pairwise analysis are adopted. Let  $\chi$  be the state variable, thus  $[\chi]$  denotes the expected values of individuals of different types at the population (e.g.  $[S_+]$  and  $[S_+I_+]$  represent the expected number of informed susceptible nodes and expected number of links connecting an informed susceptible node  
145 to an informed infected node respectively).

Therefore, with the classical mean-field approach, we can obtain:

$$\begin{aligned} \frac{d[I_+]}{dt} = & \langle k \rangle [S_+] (\sigma_S \beta [I_-] + \sigma_S \sigma_I \beta [I_+]) \\ & + \alpha [I_-] ([S_+] + [I_+]) + \omega [I_-] - \lambda [I_+] \end{aligned} \quad (1)$$

comparatively, with the pairwise approach, we can obtain:

$$\begin{aligned} \frac{d[I_+]}{dt} = & (\sigma_S \beta [S_+ I_-] + \sigma_S \sigma_I \beta [S_+ I_+]) \\ & + \alpha ([S_+ I_-] + [I_- I_+]) + \omega [I_-] - \lambda [I_+] \end{aligned} \quad (2)$$

where, the first terms of Eq.(1) and (2) describe the infection of the  $S_+$ -state individuals, the second terms describe the information acceptance of the  $I_-$ -state  
150 individuals, the third terms describe the information generation of the  $I_-$ -state individuals and the last terms represent the information loss of the  $I_+$ -state individuals. Simultaneously, the full set of differential equations based on those two approaches can be illustrated in **Appendix A**. By the way, the adaptive process could be described by the last terms of  $\frac{d[S_+ I_-]}{dt}$ ,  $\frac{d[S_- I_+] }{dt}$  and  $\frac{d[S_+ I_+]}{dt}$   
155 in the pairwise approach of Eq. (4). It should be noted that the pairwise analysis is based on a well-known closure approximation given by  $[ABC] = \frac{[AB][BC]}{[B]}$  with the assumption that the degree of each individual obeys Poisson distribution [39, 40]. In general, it might be very hard to get exact solutions of such



complex differential equations, thus we give numerical solutions of the equations  
 160 instead of the theoretical analysis in the following analysis.

### 3. Results

#### 3.1. Simulation and numerical analysis without adaptive behaviour

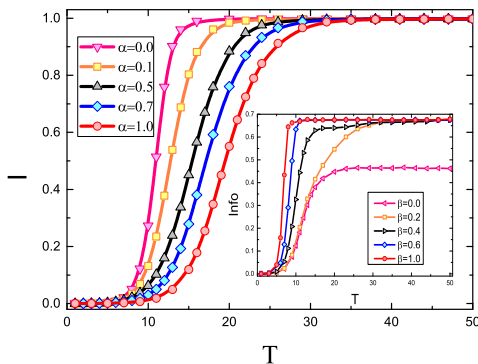


Figure 2: (Color online) The epidemic spreading dynamics of various information diffusion probabilities  $\alpha$  without considering the effect of adaptive process. The horizontal axis ( $T$ ) is the time step for the Monte Carlo simulation, the vertical axis ( $I$ ) is the density of infected (the vertical axis of the inset figure is the density of informed population in the network). The parameters are set as  $\beta = 0.3, \sigma_S = 0.5, \sigma_I = 0.7, \lambda = 0.2, \omega = 0.75, r_S = r_I = 0$ . The inset shows the information diffusion dynamics ( $Info$ ) of various  $\beta$  for  $\alpha = 0.6$ .

In this work, we perform our model on the  $ER$  network with a total population of  $N = 10000$  and average degree  $\langle k \rangle = 6$  unless otherwise stated. Moreover, all the simulation results are under 10000 realizations. We first consider a simple case of no adaptive behavior when the epidemic and disease information are spreading in the network, i.e., the case of spreading on static network. Fig. 2 gives the simulation result of the fraction of infected nodes evolving with time for various information diffusion probabilities  $\alpha$ , with the epidemic spreading probability  $\beta = 0.3$ . For the SI process, the whole population would be infected when  $\beta > 0$  for the connected social networks, resulting in that the infected density equals to 1 at last for all the values of  $\alpha$  in Fig. 2. That is to say, the  
 170

disease information diffusion cannot avoid the epidemic spreading to the whole  
 175 population when we perform our model on static network. However, we find  
 that the disease information diffusion can slow down the epidemic spreading  
 when we increase the value of  $\alpha$ . Furthermore, the time cost for the whole pop-  
 ulation becomes infected when  $\alpha = 1$  is about three times longer than that of  
 $\alpha = 0$ . In this sense, the diffusion of the disease information can slow down the  
 180 epidemic spreading significantly. In addition, the inset of Fig. 2 indicates that  
 the epidemic spreading can enhance the disease information diffusion. Actually,  
 according to model illustrated in Fig. 1, on the one hand, we can realize that  
 the epidemic spreading could be influenced by information diffusion where the  
 epidemic spreading probability of the informed individuals would change; and  
 185 on the other hand, the information diffusion could be influenced by the epidemic  
 spread where the social disease information level (namely *Info* in the inset of  
 Fig. 2) would be higher if more people are infected for the information gen-  
 eration, denoted by the parameter  $\omega$ . In this way, a mutual feedback between  
 disease spreading and information diffusion emerges: higher prevalence of the  
 190 infected individuals makes more disease information generated in the popula-  
 tion, which in turn gives rise to more informed individuals, thereby weakening  
 the spread of epidemic.

Fig. 3 shows a comparison of the evolution of infected density from the nu-  
 merical analysis according to Eq. (3) and (4) and the simulation results on *ER*  
 195 network. Infected density curve based on the classical mean-field approach is  
 much quicker than that of the simulation result, which would be caused by the  
 mean-field assumption on the SI model. In the mean-field assumption, the *I*-  
 and *S*-state individuals are well-distributed in the system. However, in the SI  
 process, the *I*-state individuals are all well clustered, resulting in that many *I*-  
 200 state individuals have no chance to contact the *S*-state individuals. In this way,  
 the classical mean-field approach can not exactly describe the SI model. How-  
 ever, such problem is not so significant in the pairwise approach, which consider  
 the time evolution of the links as well. Fig. 3 shows that the infected density  
 curve on the pairwise approach finds good agreement with the simulation results.

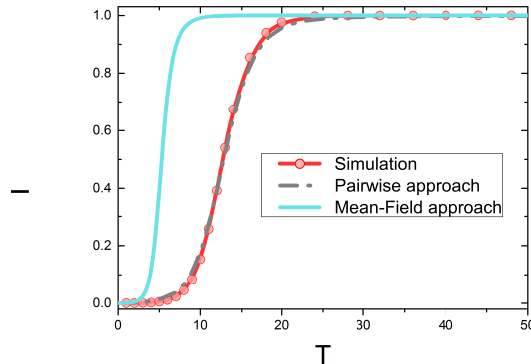


Figure 3: (Color online) Comparison of simulation results with the mean-field model and the pair approximation model without considering the effect of adaptive process. The horizontal axis ( $T$ ) is the time step for the Monte Carlo simulation, the vertical axis ( $I$ ) is the density of infected. The parameters are set as  $\beta = 0.3, \sigma_S = 0.5, \sigma_I = 0.7, \lambda = 0.2, \omega = 0.75, \alpha = 0.6, r_S = r_I = 0$ .

205

### 3.2. Spreading dynamics with the adaptive process

In this part, we shall present the spreading dynamics with the information-driven adaptive process, the results are shown in Fig. 4. Different from the results of Fig. 2, the saturation value of the infected density at the final state is much smaller than 1 in Fig. 4a. That is to say, with the adaptive process based on the information diffusion, many individuals could avoid being infected via reducing some contacts. In addition, we also plot the numerical solution based on the pairwise approach in Fig. 4a. It can be seen that the pairwise solution is not well consistent with simulation for the spreading dynamic on the adaptive network. The difference might be caused by the network structure variation in the adaptive process, where the assumption of the pairwise approach is the Poisson degree distribution. This conjecture is proved in Fig. 4b, where the degree distribution of the original network is approximate to the Poisson-distribution with mean degree around 6 (pink circle markers), while the distribution of the network at the final state (gray diamond markers) deviates from the original

210

215

220

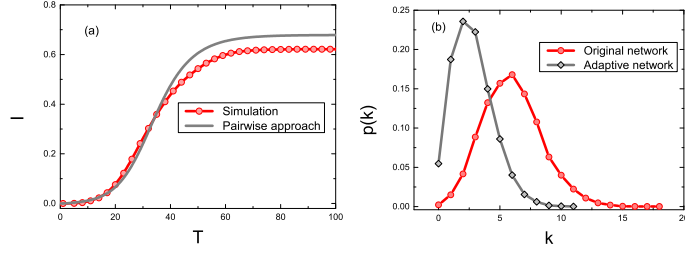


Figure 4: (Color online) Dynamical analysis of the spreading model with adaptive process. (a) Comparison of the pairwise model with the simulation results, the horizontal axis ( $T$ ) is the time step for the Monte Carlo simulation, the vertical axis ( $I$ ) is the density of infected. (b) Degree distribution of the original network and that after the adaptive process, the horizontal axis ( $k$ ) represents degree, the vertical axis ( $p(k)$ ) is degree probability. The parameters are set as  $\beta = 0.2, \sigma_S = 0.5, \sigma_I = 0.7, \lambda = 0.2, \omega = 0.2, \alpha = 0.5, r_S = 0.15, r_I = 0.1$ .

distribution. In addition, Fig. 4a shows that the difference becomes larger with the increase of time, where the degree distribution deviates more away from the original distribution when the process goes on.

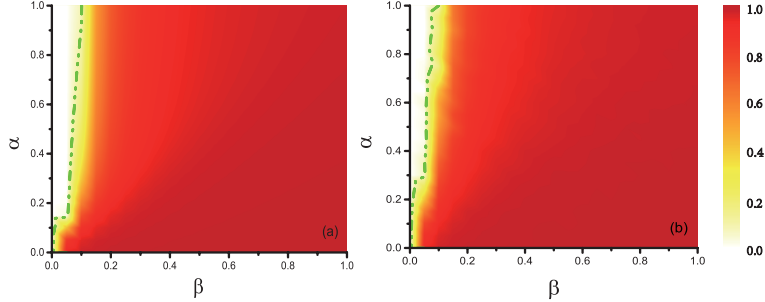


Figure 5: (Color online) The fraction of infected individuals in the stationary state (colors in the phase diagram represent the density of infected individuals at the final state, the dashed green curve shows that the prevalence value transmits from near 0 to significantly larger than 0) versus  $\alpha$  and  $\beta$  for (a) pairwise analysis and (b) simulation result. The parameters are set as  $\sigma_S = 0.5, \sigma_I = 0.7, \lambda = 0.2, \omega = 0.2, r_S = r_I = r = 0.1$ .

225 The information-driven adaptive process can not only slow down the speed of epidemic spreading, but also can diminish the epidemic prevalence at the final state significantly according to Fig. 2 and Fig. 4. For simplicity, we assume  $r_S = r_I = r$  in the following analysis. In order to exhibit the influence

of information diffusion in detail, we show the full phase diagram  $\alpha - \beta$  with  $r = 0.1$  in Fig. 5, the color gives the infected density in the final state for each combination of  $\alpha$  and  $\beta$ . The Fig. 5a and 5b are the numerical solution of the pairwise approach and the simulation result, respectively. As stated previously, the numerical solution is not very precise, but it can match the overall trend of simulation result well. For a fixed epidemic spreading probability  $\beta$ , epidemic outbreak size reduces with the increase of  $\alpha$ . That is to say, the disease information diffusion can inhibit the epidemic spreading. Analogously, the quicker and broader of the information diffusion (larger  $\alpha$ ) is, the more efficient inhibition on the epidemic spreading will be. In addition, the curve of the color mutation (the dashed green curve) in Fig. 5 could be considered as the transition point, where the epidemic can't spread out if  $\alpha$  and  $\beta$  locate at the area on the left of this curve (the white range). The threshold value of the epidemic spread probability becomes larger with the increase of  $\alpha$ .

In order to intuitively demonstrate the epidemic spreading and the information diffusion process on adaptive network, we show the simulation results of those two types of spreading processes on a  $100 \times 100$  lattice with degree  $k = 4$  in Fig. 6 for various  $\alpha$ . We present four kinds of different levels of information spreading processes (corresponding to different  $\alpha$ ), and observe how the information diffusion affects the spreading of epidemic. In addition, as the adaptive edge-breaking process is merely executed on the epidemic spreading process, while these edges can still transmit information, thus the density of informed people can still maintain at a high level in the network. For each  $\alpha$  in Fig. 6, firstly we give the fraction of the infected individuals at each time step (the red curve in each subfigure). For some particular time steps, we show the states of each individual with the gridding patterns, where the red dots and the gray dots represent the infected and informed individuals respectively (the contact networks and the un-informed susceptible individuals are not shown in the figures). We can intuitively see the distribution of the infected and informed individuals and conclude that when the diffusion of information is slower than the epidemic, we cannot stop the epidemic from spreading (Fig. 6a and 6b), however, when

the information is diffusing faster, the epidemic will be trapped into an isolated  
260 area and cannot spread anymore (Fig. 6c and 6d). Furthermore, we also give  
a visualization of these two processes on a real-word network, where we obtain  
the similar conclusion as on the lattice (see **Appendix B**).

### 3.3. Sensitivity Analysis of the model

265 **The sensitivity of the edge-breaking probability on epidemic spreading dynamics.** The phase diagram in Fig. 5 shows the impact of information diffusion rate  $\alpha$  on the epidemic spreading dynamics. In general, the adaptive edge-breaking probability  $r_S$  and  $r_I$  are also important parameters in affecting the epidemic spreading process. Fig. 7 illustrates the epidemic prevalence in  
270 the final state versus the adaptive edge-breaking rate ( $r$ ) for various information diffusion rate  $\alpha$ . It can be found that the epidemic prevalence diminishes with the increase of  $r$ , i.e., the epidemic could be controlled if people are very sensitive with the disease information and subsequently keep away from the infected. It should be noted that there is no disease information diffusion when  $\alpha = 0$ ,  
275 but with considering the information generation, the infected individuals could stop contacting with the susceptible neighbors to impede the further spreading of epidemic. With the increase of  $\alpha$ , the epidemic prevalence reduces sharply versus  $r$  and the continuous transition could be observed. By the way, it will change to a total isolation of infected individuals for  $r = 1$ , which seems to be  
280 the most effective way in controlling the contagion [41, 42].

**Dynamical characterization of the information-driven rewiring.** In order to deeply characterize the complex dynamical features of the proposed process, we concentrate on the distribution of the infected density in the final  
285 state ( $I^*$ ) rather than the simple average value [29, 36]. Fig. 8 shows four different types of dynamical behavior by calculating the distribution of the final fraction of infected for various  $\beta$  and  $r$ . For the distribution of Fig. 8a, we have carried out 10000 realizations of the infected density, and above 94% of

the infected density is 0.0001, and the maximal is 0.0007, i.e., the infected  
 290 density  $I^* \rightarrow 0$ , thus we consider this distribution indicates a healthy state (the  
 disease can't spread out) under the parameters setting here. Similarly, as to  
 the distribution of Fig. 8d, above 90% of the infected density is higher than  
 0.8, indicates a case of endemic state (epidemic outbreaks). Whereas the case  
 illustrated in Fig. 8c is very different, where the infected density  $I^*$  is around  
 295 either zero or a nonzero value. This indicates that a bistable state [29] is located  
 in this model, where healthy state and endemic state are both stable in this case.  
 In addition, a continuous dynamic behavior can also be observed in particular  
 parameter settings (Fig. 8b).

According to the dynamical behavior illustrated in Fig. 8 under different  
 300 parameter sets. Bifurcation diagram of the density of the infected as a function  
 of infected probability  $\beta$  for different values of the edge-breaking rate  $r$  is given  
 by Fig. 9a. Without the adaptive edge-breaking mechanism ( $r = 0$ ), the disease  
 can spread out only if  $\beta > 0$  for the  $SI$  process. When  $r > 0$ , the dynamical  
 behaviors become more complicated, where the discontinuous phase transitions,  
 305 bistable, oscillatory are observed. A fast edge-breaking (large  $r$ ) leads to a  
 broad healthy and bistable state range (shows by the range in the arrows) in  
 Fig. 9a. In Fig. 9b, we give a full  $r - \beta$  bifurcation diagram according to our  
 simulation results, and we can clearly identify the areas of healthy, oscillatory,  
 bistability and endemic state in this model. At last, we present the dependence  
 310 of the average value of infected density over 10,000 independent realizations on  
 $r$  and  $\beta$  in Fig. 9c, where the changing of the density is consistent with the area  
 classification in Fig. 9b.

#### 4. Conclusions

In order to understand the interplay between *the dynamics on the network*  
 315 (the spread of epidemic spreading and disease information) and *the dynamics*  
*of the network* (the time varying of network links), we present two types of  
 spreading dynamics with  $SI$  and  $SIS$  process respectively on an information-

driven adaptive network, where the individuals who have known the disease information would probably cut off their links with others. Firstly, we illustrate
   
 the mutual feedback of epidemic spreading and information diffusion without
   
 320 considering the edge-breaking process ( $r_S = r_I = 0$ ), where the high epidemic prevalence preserves high disease information level, which in turn slows down the epidemic spreading. In this case, the numerical analysis based on the pairwise approach is consistent with the simulation result very well. Secondly, the
   
 325 results are very different when the information-driven edge-breaking process is considered ( $r_S, r_I > 0$ ). The epidemic cannot spread out if the spreading probability is smaller than the threshold (shown in Fig. 5). In addition, the disease spreading and information diffusion pattern on the lattice give a visual representation that the disease might be trapped into an isolated field with
   
 information-driven adaptive process. Therefore, the information-driven adaptive process can inhibit the epidemic spreading significantly that it can not only slow down the epidemic spreading speed, but also reduce the epidemic prevalence. Finally, we give the local bifurcation analysis on four types of dynamical phenomena, including healthy, a continuous dynamic behavior, bistable and endemic, indicating that the state changes from healthy to oscillatory, bistable,
   
 330 endemic state as  $\beta$  increases.

In summary, we study the dependence of the epidemic spreading on the disease information diffusion and the information-driven adaptive process, with considering the simplest spreading model (SI) and adaptive process (edge-breaking).
   
 340 Recent researches show the different features between the epidemic and the information diffusion [43, 44, 45], and this difference dynamics would also impact the interplay between epidemic spreading and disease information diffusion significantly. Another area for future extension is to adopt other adaptation rules rather than the simple edge-breaking strategy, such as the temporarily deactivating, where the broken links would be active again after a fixed time [38] or
   
 345 if the corresponding infected node becomes recovered [37].



## 5. Acknowledgments

This work was partially supported by Natural Science Foundation of China (Grant Nos. 11305043, 11301490, 61503110, 61673151 and 11671241), Zhejiang Provincial Natural Science Foundation of China (Grant Nos. LY14A050001 and LQ16F030006), Zhejiang Qianjiang Talents Project (QJC1302001), and the EU FP7 Grant 611272 (project GROWTHCOM).

## Appendix A

Denote  $[\chi]$  as the expected values of individuals of different type described in Section 2.2, the epidemic spreading is depicted by the parameters  $\beta$ ,  $\sigma_I\beta$ ,  $\sigma_S\beta$  and  $\sigma_{SI}\beta$ , while the diffusion of disease information is controlled by the parameters:  $\alpha, \lambda, \omega$ . All these parameters have been explained in Section 2.1. According to the model described above, the the differential equations of the mean-field approach (Eq.(3)) and pairwise approach (Eq.(4)) are given as follows.

$$\left\{ \begin{array}{l} \frac{d[S_-]}{dt} = - \langle k \rangle \beta [I_-][S_-] - \langle k \rangle \sigma_I \beta [I_+][S_-] \\ \quad - \alpha([S_+] + [I_+])[S_-] + \lambda[S_+] \\ \frac{d[S_+]}{dt} = - \langle k \rangle \sigma_S \beta [I_-][S_+] - \langle k \rangle \sigma_S \sigma_I \beta [I_+][S_+] \\ \quad + \alpha([S_+] + [I_+])[S_-] - \lambda[S_+] \\ \frac{d[I_-]}{dt} = \langle k \rangle \beta [I_-][S_-] + \langle k \rangle \sigma_I \beta [I_+][S_-] \\ \quad - \alpha([S_+] + [I_+])[I_-] - \omega[I_-] + \lambda[I_+] \\ \frac{d[I_+]}{dt} = \langle k \rangle \sigma_S \beta [I_-][S_+] + \langle k \rangle \sigma_S \sigma_I \beta [I_+][S_+] \\ \quad + \alpha([S_+] + [I_+])[I_-] + \omega[I_-] - \lambda[I_+] \end{array} \right. \quad (3)$$

<i>Network</i>	<i>N</i>	<i>E</i>	<i>C</i>
Haggle	274	2124	0.0337

Table 1: Statistics of haggle network, where  $N, E, C$  represent the number of nodes, the number of links, clustering coefficient of each system respectively.

## Appendix B

We give visualization of the epidemic spreading and information diffusion with the adaptive process on a real-world network, i.e., haggle network [46]. The contacts in this network represent connection between people measured by carried wireless devices. The statistics of the network is given in Table 1. The simulation results are given in Fig. S1, which are similar to the Fig. 6.

## References

- [1] Lloyd AL, May RM. How viruses spread among computers and people. *Science* 2001;292(5520):1316–7. doi:10.1209/0295-5075/82/38004.
- [2] Danon L, Ford AP, House T, Jewell C, Keeling MJ, Roberts GO, et al. Networks and the epidemiology of infectious disease. *Interdisciplinary Perspectives on Infectious Diseases* 2011;2011:284909.
- [3] Pastor-Satorras R, Castellano C, Van Mieghem P, Vespignani A. Epidemic processes in complex networks; 2014. ArXiv: 1408.2701.
- [4] Sanz J, Xia CY, Meloni S, Moreno Y. Dynamics of interacting diseases. *Phys Rev X* 2014;4:041005.
- [5] Newman MEJ. Threshold effects for two pathogens spreading on a network. *Phys Rev Lett* 2005;95:108701.
- [6] Chen YY, Chen F, Gunnell D, Yip PSF. The impact of media reporting on the emergence of charcoal burning suicide in taiwan. *PloS ONE* 2013;8:e55000.

- [7] De Domenico M, Lima A, Mougél P, Musolesi M. The anatomy of a scientific rumor. *Sci Rep* 2013;3:2980.
- [8] Montanari A, Saberi A. The spread of innovations in social networks. *Proc Natl Acad Sci USA* 2010;107:20196–201. doi:10.1073/pnas.1004098107. 385
- [9] World Health Organization. Consensus document on the epidemiology of severe acute respiratory syndrome (SARS). World Health Organization, Geneva, Switzerland 2003;.
- [10] Tai ZX, Sun T. Media dependencies in a changing media environment: The case of the 2003 SARS epidemic in China. *New Media Soc* 2007;9:987–1009. 390
- [11] Funk S, Gilad E, Watkins C, Jansen VAA. The spread of awareness and its impact on epidemic outbreaks. *Proc Natl Acad Sci USA* 2009;106:6872–7.
- [12] Funk S, Salathé M, Jansen VAA. Modelling the influence of human behaviour on the spread of infectious diseases: a review. *J R Soc Interface* 2010;7:1247–56. 395
- [13] Granell C, Gómez S, Arenas A. Dynamical interplay between awareness and epidemic spreading in multiplex networks. *Phys Rev Lett* 2013;111:128701.
- [14] Wang Z, Andrews MA, Wu ZX, Wang L, Bauch CT. Coupled disease–behavior dynamics on complex networks: A review. *Physics of life reviews* 2015;15:1–29. 400
- [15] Wang W, Tang M, Yang H, Do Y, Lai YC, Lee G. Asymmetrically interacting spreading dynamics on complex layered networks. *Sci Rep* 2014;4:5097.
- [16] Granell C, Gómez S, Arenas A. Competing spreading processes on multiplex networks: Awareness and epidemics. *Phys Rev E* 2014;90:012808.
- [17] Funk S, Gilad E, Jansen VAA. Endemic disease, awareness, and local behavioural response. *J Theor Bio* 2010;264:501–9. 405

- [18] Sahneh FD, Chowdhury FN, Scoglio CM. On the existence of a threshold for preventive behavioral responses to suppress epidemic spreading. *Sci Rep* 2012;2:632.
- 410 [19] Zhang HF, Wu ZX, Tang M, Lai YC. Effects of behavioral response and vaccination policy on epidemic spreading - an approach based on evolutionary-game dynamics. *Sci Rep* 2014;4:5666.
- [20] Wu QC, Fu XC, Small M, Xu XJ. The impact of awareness on epidemic spreading in networks. *Chaos* 2012;22:013101.
- 415 [21] Funk S, Jansen VA. Interacting epidemics on overlay networks. *Physical Review E* 2010;81(3):036118.
- [22] Marceau V, Noël PA, Hébert-Dufresne L, Allard A, Dubé LJ. Adaptive networks: Coevolution of disease and topology. *Physical Review E* 2010;82(3):036116.
- 420 [23] Barabási AL, Albert R. Emergence of scaling in random networks. *Science* 1999;286:509–12. doi:10.1126/science.286.5439.509.
- [24] Watts DJ, Strogatz SH. Collective dynamics in ‘small-world’ networks. *Nature* 1998;393:440–2.
- [25] Holme P, Saramäki J. Temporal networks. *Phys Rep* 2012;519:97–125.
- 425 [26] Pastor-Satorras R, Vespignani A. Epidemic spreading in scale-free networks. *Phys Rev Lett* 2001;86:3200. doi:10.1103/PhysRevLett.86.3200.
- [27] Liu C, Zhang ZK. Information spreading on dynamic social networks. *Commun Nonlinear Sci Numer Simulat* 2014;19(4):896–904.
- [28] Gracia-Lázaro C, Ferrer A, Ruiz G, Tarancón A, Cuesta JA, Sánchez A, et al. Heterogeneous networks do not promote cooperation when humans play a Prisoner’s Dilemma. *Proc Natl Acad Sci USA* 2012;109:12922–6.
- 430

- [29] Gross T, D’Lima CJD, Blasius B. Epidemic dynamics on an adaptive network. *Phys Rev Lett* 2006;96:208701. doi:10.1103/PhysRevLett.96.208701.
- 435 [30] Gross T, Blasius B. Adaptive coevolutionary networks: a review. *J R Soc Interface* 2008;5:259–71.
- [31] Gross T, Sayama H. *Adaptive networks*. Berlin: Springer; 2009.
- [32] Tunc I, Shaw LB. Effects of community structure on epidemic spread in an adaptive network. *Phys Rev E* 2014;90:022801.
- 440 [33] Zhou YZ, Xia YJ. Epidemic spreading on weighted adaptive networks. *Physica A* 2014;399:16–23.
- [34] Volz E, Meyers LA. Susceptible-infected-recovered epidemics in dynamic contact networks. *Proc R Soc B* 2007;274:2925–33. doi:10.1098/rspb.2007.1159.
- 445 [35] Wieland S, Aquino T, Nunes A. The structure of coevolving infection networks. *EPL (Europhys Lett)* 2012;97:18003. doi:10.1209/0295-5075/97/18003.
- [36] Guo DC, Trajanovski S, van de Bovenkamp R, Wang HJ, Van Mieghem P. Epidemic threshold and topological structure of susceptible-infectious-susceptible epidemics in adaptive networks. *Phys Rev E* 2013;88:042802.
- 450 [37] Tunc I, Shkarayev MS, Shaw LB. Epidemics in adaptive social networks with temporary link deactivation. *J Stat Phys* 2013;151:355–66.
- [38] Valdez LD, Macri PA, Braunstein LA. Intermittent social distancing strategy for epidemic control. *Phys Rev E* 2012;85:036108.
- 455 [39] Morris AJ. Representing spatial interactions in simple ecological models. Ph.D. thesis; University of Warwick; 1997.

- [40] Keeling MJ. The effects of local spatial structure on epidemiological invasions. *Proc R Soc London, Ser B* 1999;266:859–67.
- [41] Crokidakis N, Queirós SMD. Probing into the effectiveness of self-isolation policies in epidemic control. *J Stat Mech* 2012;:P06003.  
460
- [42] Lagorio C, Dickison M, Vazquez F, Braunstein LA, Macri PA, Migueles MV, et al. Quarantine-generated phase transition in epidemic spreading. *Phys Rev E* 2011;83:026102.
- [43] Lü L, Chen DB, Zhou T. The small world yields the most effective information spreading. *New J Phys* 2011;13:123005. doi:10.1088/1367-2630/13/12/123005.  
465
- [44] Zhang ZK, Zhang CX, Han XP, Liu C. Emergence of blind areas in information spreading. *PLoS ONE* 2014;9(4):e95785.
- [45] Cai W, Chen L, Ghanbarnejad F, Grassberger P. Avalanche outbreaks emerging in cooperative contagions. *Nature physics* 2015;11(11):936–40.  
470
- [46] Chaintreau A, Hui P, Crowcroft J, Diot C, Gass R, Scott J. Impact of human mobility on opportunistic forwarding algorithms. *IEEE Transactions on Mobile Computing* 2007;6(6):606–20.

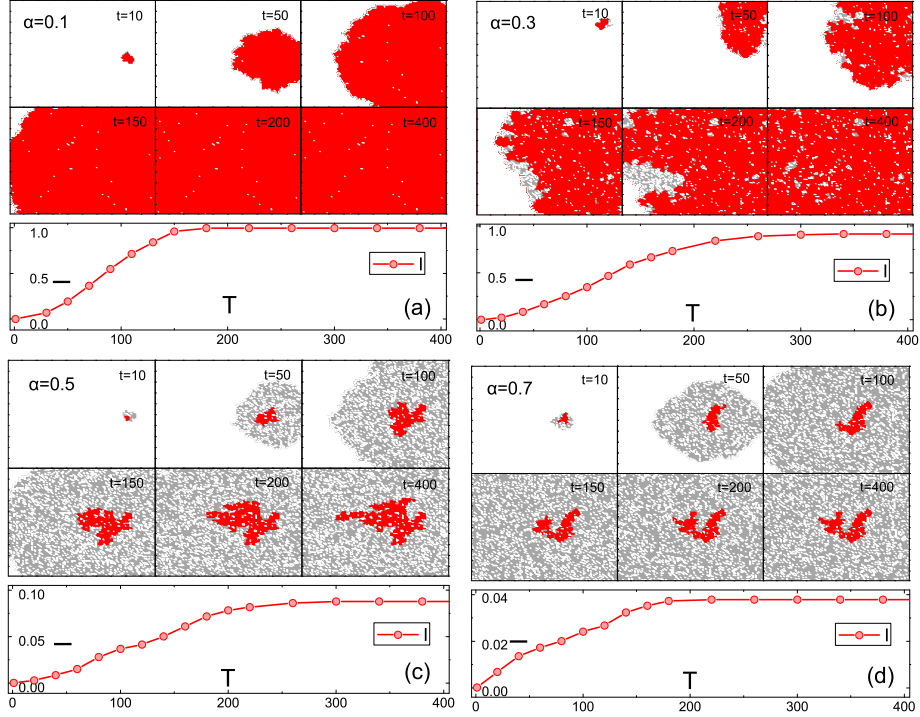


Figure 6: (Color online) Illustration to dynamic spreading process by considering the adaptive effect on the lattice. The square gridding patterns show the distribution of the infected and informed individuals in some particular time steps. The red area represents the nodes that are infected by the epidemic, while the gray area represents the informed individuals. The red curves (lower panels) describe the fraction of infected individuals over time with corresponding (the horizontal axis ( $T$ ) is the time step for the Monte Carlo simulation, the vertical axis ( $I$ ) is the density of infected). (a)  $\alpha = 0.1$ ; (b)  $\alpha = 0.3$ ; (c)  $\alpha = 0.5$ ; (d)  $\alpha = 0.7$ . Other parameters are set as  $\beta = 0.4, \sigma_S = 0.4, \sigma_I = 0.8, \lambda = 0.1, \omega = 0.2, r_S = r_I = r = 0.1$ .

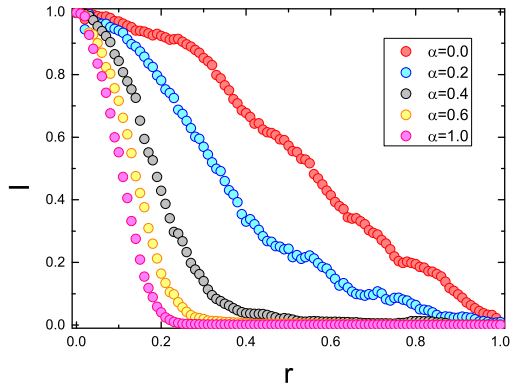


Figure 7: (Color online) Fraction of infected individuals versus  $r$ . Different curves correspond to different  $\alpha$ . Other parameters are set as  $\beta = 0.2, \sigma_S = 0.5, \sigma_I = 0.7, \lambda = 0.2, \omega = 0.2$ .

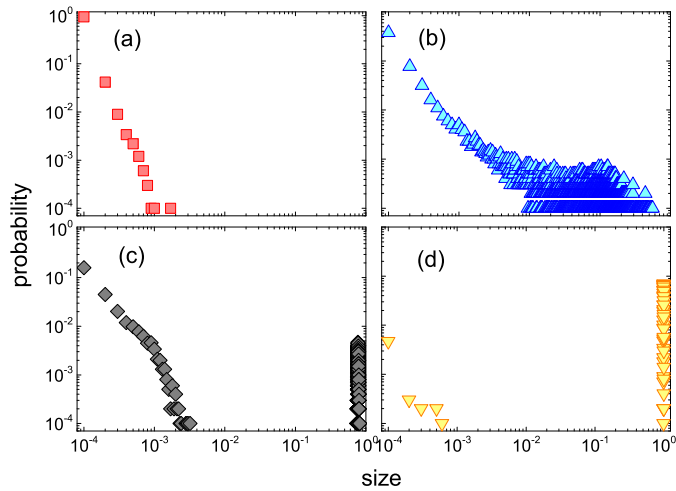


Figure 8: (Color online) Distribution of the infected density in the final state versus different values of  $r$  and  $\beta$ . Each distribution is obtained by carrying out 10,000 independent realizations for the final fraction of infected. The parameters are set as  $r_S = r_I = r = 0.7, 0.35, 0.15, 0$ ;  $\beta = 0.05, 0.35, 0.25, 0.4$  for (a), (b), (c) and (d) respectively. Other parameters are  $\sigma_S = 0.5, \sigma_I = 0.7, \lambda = 0.2, \omega = 0.2, \alpha = 0.6$ .



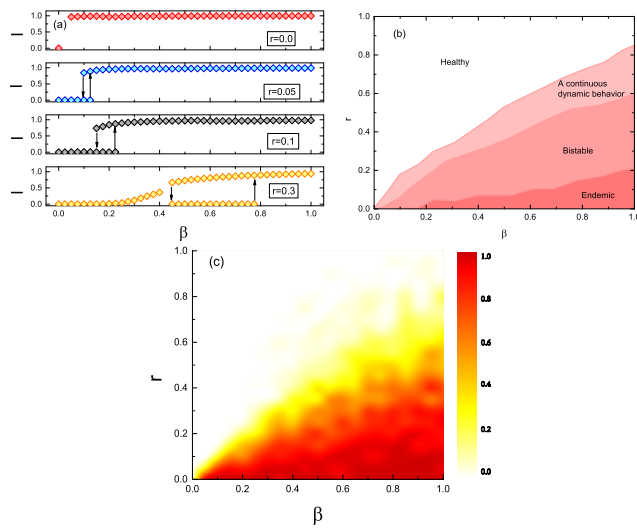


Figure 9: (Color online) (a) Bifurcation diagram of the density of the infected  $I$  as a function of the infection probability  $\beta$  for different values of the edge-breaking rate  $r$  based on the results of simulation of the full network (diamonds). (b) Two parameter bifurcation diagram showing the dependence on the edge-breaking rate  $r$  and the infection probability  $\beta$  based on the results of simulation of the full network. (c) Full phase diagram  $r - \beta$  for the simulation of the adaptive process. The parameters are the same as Fig. 8.

$$\begin{aligned}
\frac{d[S_-]}{dt} &= -\beta[S_-I_-] - \sigma_I\beta[S_-I_+] - \alpha([S_-S_+] + [S_-I_+]) + \lambda[S_+] \\
\frac{d[S_+]}{dt} &= -\sigma_S\beta[S_+I_-] - \sigma_S\sigma_I\beta[S_+I_+] + \alpha([S_-S_+] + [S_-I_+]) - \lambda[S_+] \\
\frac{d[I_-]}{dt} &= \beta[S_-I_-] + \sigma_I\beta[S_-I_+] - \alpha([S_+I_-] + [I_-I_+]) - \omega[I_-] + \lambda[I_+] \\
\frac{d[I_+]}{dt} &= \sigma_S\beta[S_+I_-] + \sigma_S\sigma_I\beta[S_+I_+] + \alpha([S_+I_-] + [I_-I_+]) + \omega[I_-] - \lambda[I_+] \\
\frac{d[S_-I_-]}{dt} &= -\beta[S_-I_-] + \lambda([S_+I_-] + [S_-I_+]) - \omega[S_-I_-] + \beta\frac{[S_-I_-]([S_-S_-] - [S_-I_-])}{[S_-]} + \sigma_I\beta\frac{[S_-I_+]([S_-S_-] - [S_-I_-])}{[S_-]} \\
&\quad - \alpha\frac{[S_-I_-]([S_-I_+] + [S_-S_+])}{[S_-]} - \alpha\frac{[S_-I_-]([I_-I_+] + [S_+I_-])}{[I_-]} \\
\frac{d[S_-I_+]}{dt} &= -\sigma_I\beta[S_-I_+] + \omega[S_-I_-] + \lambda[S_+I_+] - \alpha[S_-I_+] - \lambda[S_-I_+] - \beta\frac{[S_-I_-][S_-I_+]}{[S_-]} - \sigma_I\beta\frac{[S_-I_+]^2}{[S_-]} + \sigma_S\beta\frac{[S_+I_-][S_-S_+]}{[S_+]} \\
&\quad + \sigma_S\sigma_I\beta\frac{[S_+I_+][S_-S_+]}{[S_+]} + \alpha\frac{[S_-I_-]([I_-I_+] + [S_+I_-])}{[I_-]} - \alpha\frac{[S_-I_+]([S_-I_+] + [S_-S_+])}{[S_-]} - r_I[S_-I_+] \\
\frac{d[S_+I_-]}{dt} &= -\sigma_S\beta[S_+I_-] + \lambda[S_+I_+] - \lambda[S_+I_-] - \alpha[S_+I_-] - \omega[S_+I_-] - \sigma_S\beta\frac{[S_+I_-]^2}{[S_+]} - \sigma_S\sigma_I\beta\frac{[S_+I_+][S_+I_-]}{[S_+]} + \beta\frac{[S_-I_-][S_-S_+]}{[S_-]} \\
&\quad + \sigma_I\beta\frac{[S_-I_+][S_-S_+]}{[S_-]} + \alpha\frac{[S_-I_-]([S_-S_+] + [S_-I_+])}{[S_-]} - \alpha\frac{[S_+I_-]([I_-I_+] + [S_+I_-])}{[I_-]} - r_S[S_+I_-] \\
\frac{d[S_+I_+]}{dt} &= -\sigma_S\sigma_I\beta[S_+I_+] + \alpha[S_-I_+] + \alpha[S_+I_-] + \omega[S_+I_-] - 2\lambda[S_+I_+] + \sigma_S\beta\frac{[S_+I_-]([S_+S_+] - [S_+I_+])}{[S_+]} \\
&\quad + \sigma_S\sigma_I\beta\frac{[S_+I_+]([S_+S_+] - [S_+I_+])}{[S_+]} + \alpha\frac{[S_-I_+]([S_-I_+] + [S_-S_+])}{[S_-]} + \alpha\frac{[S_+I_-]([S_+I_-] + [I_-I_+])}{[I_-]} - [1 - (1 - r_S)(1 - r_I)][S_+I_+] \\
\frac{d[I_-I_-]}{dt} &= 2\beta[S_-I_-] + 2\lambda[I_-I_+] - 2\omega[I_-I_-] + 2\beta\frac{[S_-I_-]^2}{[S_-]} + 2\sigma_I\beta\frac{[S_-I_+][S_-I_-]}{[S_-]} - 2\alpha\frac{[I_-I_-]([S_+I_-] + [I_-I_+])}{[I_-]} \\
\frac{d[I_-I_+]}{dt} &= \sigma_I\beta[S_-I_+] + \sigma_S\beta[S_+I_-] + \omega([I_-I_-] - [I_-I_+]) + \lambda([I_+I_+] - [I_-I_+]) - \alpha[I_-I_+] + \beta\frac{[S_-I_-][S_-I_+]}{[S_-]} + \sigma_I\beta\frac{[S_-I_+]^2}{[S_-]} \\
&\quad + \sigma_S\beta\frac{[S_+I_-]^2}{[S_+]} + \sigma_S\sigma_I\beta\frac{[S_+I_+][S_+I_-]}{[S_+]} + \alpha\frac{[I_-I_-]([S_+I_-] + [I_-I_+])}{[I_-]} - \alpha\frac{[I_-I_+]([S_+I_-] + [I_-I_+])}{[I_-]} \\
\frac{d[I_+I_+]}{dt} &= 2\sigma_S\sigma_I\beta[S_+I_+] + 2\alpha[I_-I_+] + 2\omega[I_-I_+] - 2\lambda[I_+I_+] + 2\sigma_S\beta\frac{[S_+I_-][S_+I_+]}{[S_+]} + 2\sigma_S\sigma_I\beta\frac{[S_+I_+]^2}{[S_+]} + 2\alpha\frac{[I_-I_+]([S_+I_-] + [I_-I_+])}{[I_-]} \\
\frac{d[S_-S_-]}{dt} &= 2\lambda[S_-S_+] - 2\beta\frac{[S_-I_-][S_-S_-]}{[S_-]} - 2\sigma_I\beta\frac{[S_-I_+][S_-S_-]}{[S_-]} - 2\alpha\frac{[S_-S_-]([S_-S_+] + [S_-I_+])}{[S_-]} \\
\frac{d[S_-S_+]}{dt} &= \lambda[S_+S_+] - \lambda[S_-S_+] - \alpha[S_-S_+] - \sigma_S\beta\frac{[S_+I_-][S_-S_+]}{[S_+]} - \sigma_S\sigma_I\beta\frac{[S_+I_+][S_-S_+]}{[S_+]} - \beta\frac{[S_-I_-][S_-S_+]}{[S_-]} - \sigma_I\beta\frac{[S_-I_+][S_-S_+]}{[S_-]} \\
&\quad + \alpha\frac{[S_-S_-]([S_-S_+] + [S_-I_+])}{[S_-]} - \alpha\frac{[S_-S_+]([S_-S_+] + [S_-I_+])}{[S_-]} \\
\frac{d[S_+S_+]}{dt} &= 2\alpha[S_-S_+] - 2\lambda[S_+S_+] - 2\sigma_S\beta\frac{[S_+I_-][S_+S_+]}{[S_+]} - 2\sigma_S\sigma_I\beta\frac{[S_+I_+][S_+S_+]}{[S_+]} + 2\alpha\frac{[S_-S_+]([S_-S_+] + [S_-I_+])}{[S_-]} \\
&\quad (4)
\end{aligned}$$

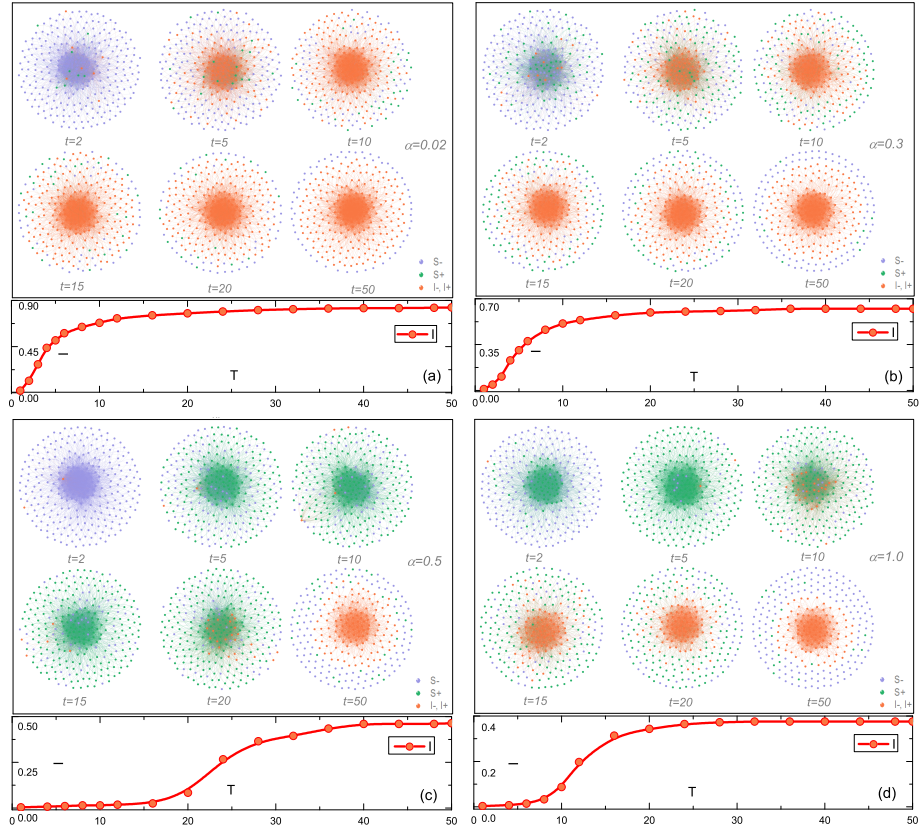


Figure 10: (Color online) Illustration to dynamic spreading process by considering the adaptive effect on hagggle network, while the purple, green and red circles represent individuals in  $S_-$ ,  $S_+$  and  $I$  state respectively. The red curves (lower panels) describe the fraction of infected individuals over time with corresponding parameters. (a)  $\alpha = 0.02$ ; (b)  $\alpha = 0.3$ ; (c)  $\alpha = 0.5$ ; (d)  $\alpha = 1.0$ . Other parameters are set as  $\beta = 0.1, \sigma_S = 0.3, \sigma_I = 0.5, \lambda = 0.08, \omega = 0.2, r_S = r_I = r = 0.08$ .